Pure Appl. Chem., Vol. 76, No. 4, pp. 815–828, 2004.

Selective control and rate enhancement of reactions involving catalytic reduction of organohalides and reduced form of myoglobin in microemulsions*

Geoffrey N. Kamau[2,‡] and Bernard Munge[1]

[1]Department of Chemistry, Box U-60, University of Connecticut, Storrs, CT 06269-3060, USA; [2]Department of Chemistry, University of Nairobi, P.O. Box 30197, Nairobi, Kenya

Abstract: Myoglobin (horse heart, Mb) adsorbed on carbon electrodes or in solution at platinum electrodes was used for electrocatalytic reduction of *trans*-1,2-dibromocyclohexane (DBCH) and trichloroacetic acid (TCA) in a bicontinuous microemulsion, prepared from sodium didodecyl sulfate (SDS) or hexadecyltrimethylammonium bromide (CTAB), tetradecane, pentanol, and water. Carbon electrodes (glassy carbon, GC, and pyrolytic graphite, PG) exhibited adsorption peaks, whereas platinum (Pt) portrayed diffusion-controlled peaks. Electrode reduction of Mb had $E^{0\prime}$ at –0.179 ± 0.013 V at GC/SDS, –0.189 ± 0.015 at GC/CTAB, and –0.562 ± 0.018 at Pt/SDS and 0.611 ± 0.008 at Pt/CTAB media. Current efficiencies for electrocatalytic reduction of TCA were higher than that for reduction of dibromocyclohexane. For both substrates, dibromocyclohexane and trichhloroacetic acid, a lowering of overpotential of at least 1.3 V was achieved. Overall, the Pt electrode exhibited higher catalytic efficiencies compared to carbon electrodes, suggesting higher surface concentration and unhindered orientation of the substrate on the Pt electrode. For DBCH, catalytic efficiencies decreased with scan rate, at carbon electrodes as expected for homogeneous solutions, whereas an average value of 2.22 ± 0.42 in SDS and 3.29 ± 0.76 in CTAB microemulsion was obtained at Pt electrodes at a scan rate range of 15 to 3000 mV s^{-1}. Pseudo-first-order rate constants (k') for the rate-determining step (rds) involving reaction of organohalides with catalyst had an average value of 41 ± 1 M^{-1} s^{-1} for reduction of DBCH/SDS and $4.8 \pm 1.0 \times 10^2$ M^{-1} s^{-1} for reduction of TCA/SDS. Moreover, rate constants were higher in CTAB microemulsion, giving values of $1.5 \pm 0.016 \times 10^2$ and $2.75 \pm 0.67 \times 10^3$ M^{-1} s^{-1} for DBCH and TCA, respectively. Positive interfacial charge of the microemulsion conduits influenced catalytic reaction of catalyst and the substrate. Under the conditions of the experiment, no hydrogen evolution was observed at Pt electrodes.

INTRODUCTION

The use of surfactants to bring oil and water together produces a "new" class of solubilization media, in this case known as bicontinuous microemulsion [1]. Microemulsions are less toxic and less expensive than the conventional organic solvents commonly used to dissolve nonpolar molecules, specifically needed for synthesis in industries and destruction of organohalide pollutants [2]. This is in line with the

*Plenary lecture presented at the Southern and Eastern Africa Network of Analytical Chemists (SEANAC), Gaborone, Botswana, 7–10 July 2003. Other presentations are published in this issue, pp. 697–888.

‡Corresponding author

public health outcry for the use of more friendly, less toxic media in the environment. Moreover, microemulsions can be used to mimic enzyme fluids found in biological systems [3,4]. Bicontinuous microemulsions are clear, stable mixtures consisting of conduits of oil and water, with the interfacial site occupied by surfactants and cosurfactants, in this case alcohol, which has a number of applications [2,5,6]. Previously, these microheterogeneous and macrohomogeneous fluids were used to control and enhance rates of electrode-mediated catalytic reactions [6–9]. For example, improved catalytic efficiencies were obtained in bicontinuous microemulsions relative to homogeneous solvent for reduction of nonpolar organohalide substrates, but not for the polar trichloroacetic acid [6,9]. Effective formulation of pesticides using halide functional groups has caused organohalides to be major pollutants, with varying degrees of toxicity, within our environment. The enhanced observed rates for decomposition of these organohalides, using appropriate mediators, were attributed to preconcentration of nonpolar reactants in coadsorbed layer of surfactant and the catalyst on the surface of the electrode. Such preconcentration steps were also observed in micellar solutions [6,10,11].

Bicontinuous microemulsions can be prepared by using double chain alkylammonium surfactants and appropriate amounts of oil and water [9,12–14]. It may also be prepared using single chain alkylammonium surfactants like cetyltrimethylammonium bromide (CTAB) or sodium didodecyl sulfate (SDS), suitable oil, cosurfactant, and water. The ratio of participating components can be varied accordingly for specific applications. The ability of the experimentalist to engineer the microenvironment for selected reaction, using microemulsions, provides a major breakthrough in a variety of applications, such as electrosynthesis, related industrial applications, and environmental control measures.

The heme protein myoglobin (Mb) is responsible for oxygen transport in muscles of biological systems. However, Mb can catalyze organic oxidations [15–17] and reductions [18–21], similar to the heme enzyme cytochrome P450 [22]. Catalytic decomposition of organohalides by reduced iron porphyrins and other heme-like transition-metal complexes has been studied extensively. In the case of vicinal dihalides, these reactions involve two-electron transfer, giving olefins as the main product [23–25]. Examples include conversion of ethylene dibromide to ethylene [26–30] or trichloroacetic acid to acetic acid [26,31]. Earlier work demonstrated direct electron transfer between electrodes and aquo-metmyoglobin in insoluble, ordered, liquid-crystal surfactant films [26,32–34]. The Fe(II) of Mb can be oxidized to form metmyoglobin (metMb). MetMb does not bind oxygen molecule, since its Fe(III) is already octahedrally coordinated with a water molecule in the sixth position (Sketch 1). MetMb has the characteristic brown color seen in dried blood and old meat [35].

In this paper we compare the reduction of *trans*-1,2-dibromocyclohexane (DBCH) and trichloroacetic acid catalyzed by Mb in both anionic and cationic bicontinuous microemulsions at carbon (glassy carbon, GC, and pyrolytic graphite, PG) and Pt electrodes. Previous work had indicated limitations of electrocatalytic reduction of organohalides by Mb in homogeneous solutions [26]. However, the present work demonstrates electrode reduction of Mb and catalytic decomposition of organohalides in bicontinuous anionic and cationic microemulsions and extension of the working range of Pt electrode prior to hydrogen evolution. The quantities of constituents used for preparing the current microemulsions are relatively cost-effective and have been described previously [34]. It was also the aim of this work to investigate the adsorption phenomenon on the surface of the electrode and the influence of the surfactant charge on the electrode reactions.

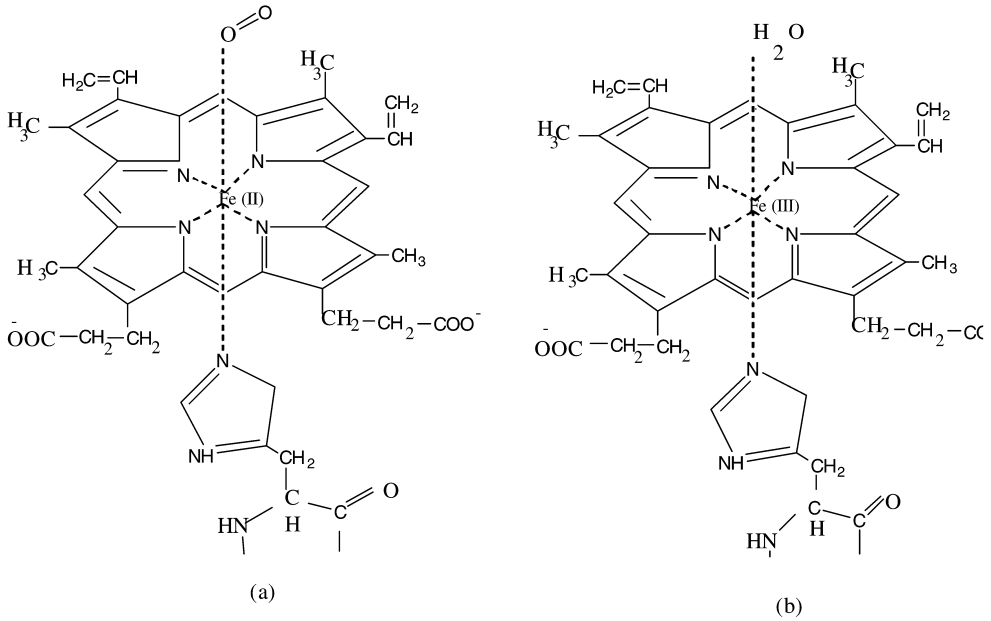

Sketch 1 (a) Heme (ferroprotoporphyrin) liganded to His and oxygen; (b) Heme (ferriprotoporphyrin) liganded to His and water: example of oxidized form of MetMb.

EXPERIMENTAL SECTION

Chemicals and solutions

Cetyltrimethylammonium bromide (CTAB, 99 %), sodium dodecyl sulfate (SDS, 99 %), and tetradecane were from Acros and were used as received. Horse skeletal muscle myoglobin from Sigma was dissolved in a pH 4.6 buffer (0.01 M acetate titrated with acetic acid) containing 0.05 M NaCl or in a pH 4.6 SDS (13 %) microemulsion containing 0.1 M NaCl or in CTAB (5 %) microemulsions. Microemulsions were prepared by mixing the following components (% weight): 13 % SDS was added to stirred water (52 %) solution containing 0.1 M NaCl. This was then titrated with 27 % *n*-pentanol, followed by 8 % tetradecane. 5 % CTAB was added to stirred 88.6 % water, then titrated with 5.4 % *n*-pentanol and 1 % tetradecane. Trichloroacetic acid (TCA) was from Janssen Chimical. *Trans*-1,2-dibromocyclohexane, tetradecane, and pentanol were from Aldrich. Water was purified with Hydro Service & Supplies equipment to a specific resistance >18 MΩ–cm. All other chemicals were reagent grade.

Apparatus

A CHI 660 and 430 Workstation (CHI Instruments) was used for cyclic voltammetry and bulk electrolysis. A three-electrode cell was used with saturated calomel electrode (SCE) as reference electrode. A platinum wire was used as the counter electrode and PG (0.17 cm^2) or GC (0.10 cm^2) with or without adsorbed Mb or platinum disk (0.018 cm^2) were used as the working electrodes. All experiments were performed at ambient temperature (22 ± 2 °C), except for bulk electrolysis, which was done at 4 °C.

Voltammetry on electrodes containing preadsorbed metMb was done in acetate buffer (pH 4.6) or in microemulsions. All solutions (5 ml) were purged with pure nitrogen gas for at least 25 min prior to initiation of the experiment. A nitrogen-saturated environment was then maintained during experimental runs. Initially, all electrodes were polished with 400-, 600-grit silicon carbide paper (Carbimet), then

0.3 μm alumina on Mark V Laboratory green billiard cloth on a polishing wheel for a minute, followed by ultrasonication. Water was applied during each polishing step. Later, for each experimental run at Pt electrode the electrode was polished on Buehler green cloth (1 min) followed by rinsing in water and drying in a nitrogen atmosphere.

RESULTS

UV–vis spectroscopy

Absorption spectra of Mb, pH 4.6, acetate buffer gave a characteristic band with λ_{max} 409 (Fig. 1), similar to what was reported earlier [36–38]. However, in SDS microemulsion, pH 4.6, a blue shift in absorption band occurred, giving a peak at λ_{max} 401, similar to what was observed in CTAB microemulsion [36b], suggesting surface charge on the surfactant does not influence the soreto band significantly. Moreover, in *n*-pentanol a band occurred at λ_{max} 401. Since Mb does not dissolve in tetradecane, these results indicate that Mb resides in the interstitial sites of the microemulsion and not in the water channel alone.

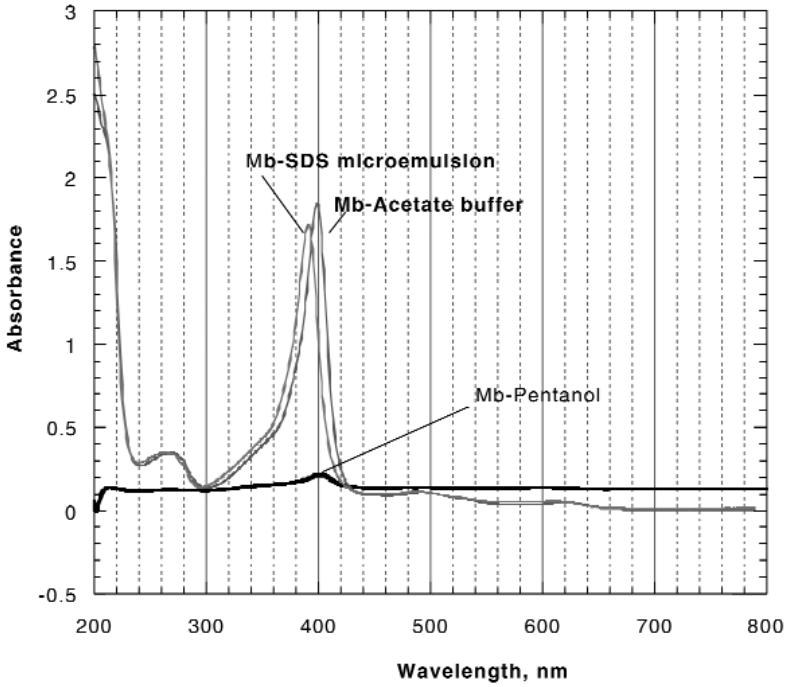

Fig. 1 UV–vis spectra of metMb (7 μM) acetate buffer (pH 4.6), SDS microemulsion (pH 4.6), and *n*-pentanol.

Voltammetry

The bicontinuous SDS/water/tetradecane/pentanol (13:52:8:27) and CTAB/water/tetradecane/pentanol (5:88.6:1:5.4) microemulsions chosen for this work had been characterized previously by conductivity, viscosity, and diffusion methods [39–42]. These studies showed that these fluids are continuous in both oil and water. In order to relatively retain the nativity of Mb, the solutions were initially prepared in acetate buffer (pH 4.6) or in SDS microemulsion (pH 4.6), then diluted to the required concentrations in the appropriate media. Cyclic voltammograms of 0.07 mM in anaerobic SDS microemulsion at a polished basal plane PG electrodes gave a reduction peak at –0.268 V vs. SCE and an oxidation peak cen-

tered around –0.18 V vs. SCE (Fig. 2). The peaks represents the MbFe(III)/Fe(II) redox couple, as reported previously [26,31,43]. Similarly, reduction of metMb at GC electrode in SDS microemulsion gave a reduction peak at –0.23 V and an oxidation peak at –0.21 V vs. SCE. The peak separation (Epa-Epc) was less than 60, at low scan rates, suggesting adsorption phenomenon. Adsorption of Mb at carbon electrodes was confirmed by the shape of voltammograms and a plot of current (I_p) vs. scan rate, which gave a linear relationship [44]. A nonlinear relationship was obtained for a plot of I_p vs. $\upsilon^{1/2}$, where υ is the scan rate in mV s^{-1}. Scan rate studies (υ = 25–800 mV s^{-1}) at GC-SDS system did not show any significant peak shift (Fig. 3). Similar results were obtained in CTAB microemulsions, except that reduction peaks shifted slightly. On the other hand, reduction of Mb at Pt electrode in SDS microemulsions gave a reduction peak at –0.57 V vs. SCE and an oxidation peak at –0.48 V of equal magnitude (Fig. 3b). The peak separation was 60 mV at low scan rates, suggesting diffusion-controlled conditions. For this electrode, peak currents were proportional to $\upsilon^{1/2}$, in the range of 25 to 3000 mV s^{-1}, as expected for diffusion-controlled electrode process [44]. The high current densities and diffusion coefficients observed for this electrode are consistent with the formation of a thick Mb-surfactant film on Pt electrode, through which Mb diffuses.

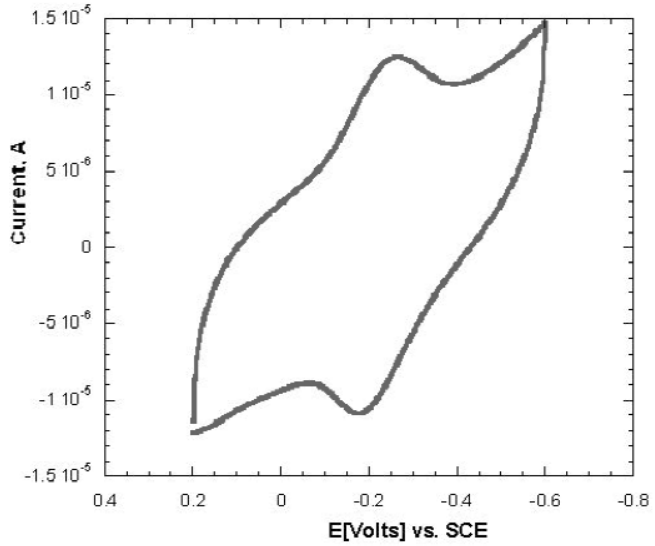

Fig. 2 Cyclic voltammogram of 0.07 mM metMb in SDS microemulsion at 0.3 V s^{-1} on polished pyrolytic graphite.

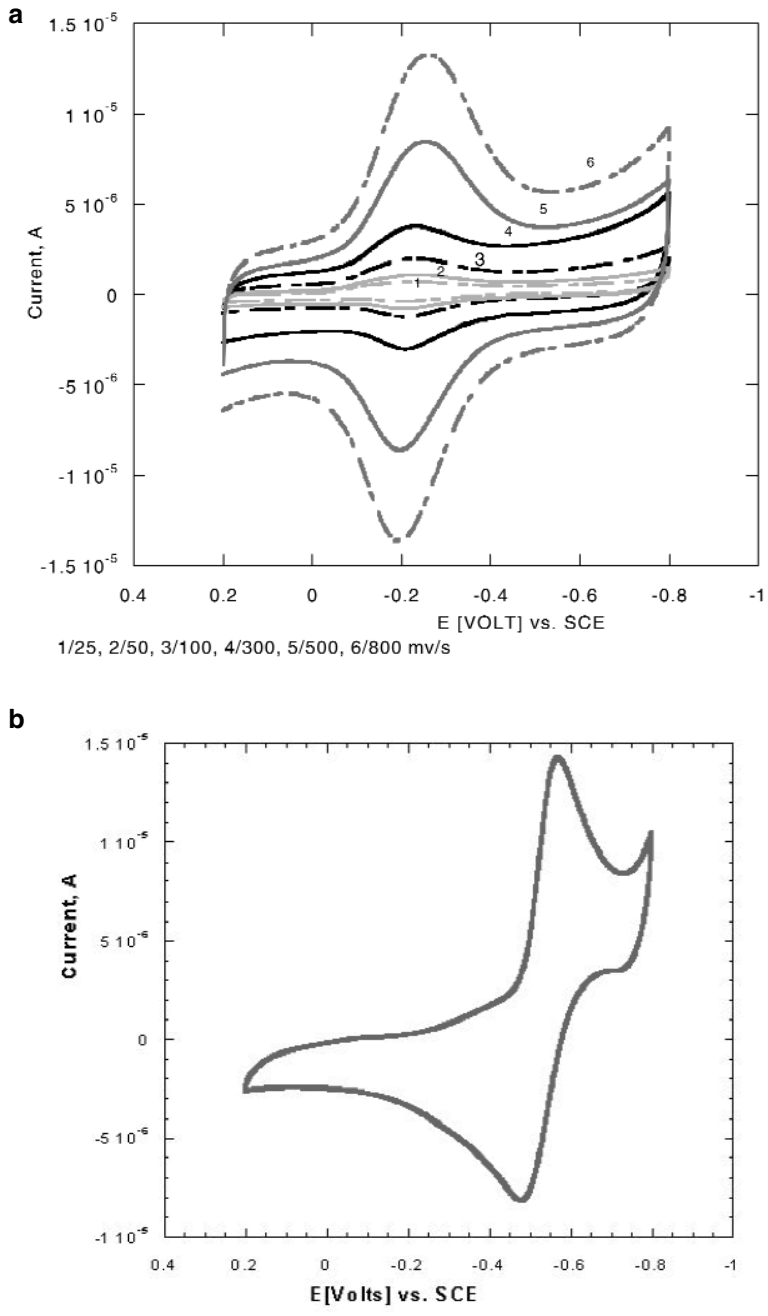

Fig. 3 (a) Variation of cathodic current of metMbFe(III)/Fe(II) couple with scan rate in SDS microemulsions at glassy carbon electrode: 1 = 0.025 V s^{-1}, 2 = 0.05 V s^{-1}, 3 = 0.1 V s^{-1}, 4 = 0.3 V s^{-1}, 5 = 0.5 V s^{-1}, 6 = 0.8 V s^{-1}; (b) Cyclic voltammogram of 0.07 mM metMb in SDS microemulsion at 0.3 V s^{-1}, Pt electrode.

Adsorption

Voltammograms indicated that the adsorbed Mb layers at GC and PG electrodes were stable in SDS and CTAB microemulsions and acetate buffer solution for several days, even when there was no Mb in the solution. When the previously used electrodes were used in fresh microemulsions or acetate buffer, Mb peaks were still detectable. For GC and PG to be used for new experiments, extensive polishing, starting from 400-grit silicon carbide papers, was necessary to removed the adsorbed layers of myoglobin. Overall, results at carbon electrodes suggest that the main reduction wave of MbFe(III)/Fe(II) redox couple consists of electrode surface-bound species, which demonstrates a case of thin-layer electrochemistry. This is further supported by the fact that voltammograms obtained in a stirred solution, involving nitrogen flow, did not show significant variation in current-potential curve.

Electrode parameters

The apparent standard heterogeneous rate constant for electron transfer ($k^{o'}$) and formal potentials for the MbFe(III)/Fe(II) redox couples were obtained from CV data (Table 1) by using standard procedures [44]. Diffusion coefficient could only be obtained in case of Pt electrodes, since diffusion occurred within the thick films of the surfactant layers on the surface of the electrode. Moreover, electron-transfer rate constant ($k^{o'}$) for the MbFe(III)/Fe(II) couples were higher than those obtained in aqueous acetate buffer solutions [43,45]. Former potentials taken as potentials at a 85.17 % peak current (CV) were slightly more positive for the MetMbFe(III)/Fe(II) couples in SDS than in CTAB. This may be attributed to the size and the type of charge on the two hydrophobic chains of the microemulsions. Normally, one would expect the positive charge on CTAB to stabilize the reduced species of the MbFe(III)/Fe(II) couple, which is not the case here, suggesting that the size of the hydrocarbon chain outweighs the electrostatic forces. Sufficient reversibility in CV of the MbFe(III)/Fe(II) couple at scan rates above 100 mV s^{-1} but less than 3000 mV s^{-1} was obtained to estimate formal potentials and heterogeneous rate constants in SDS and CTAB microemulsions. Theoretical curves were constructed (Fig. 4) and used to estimate the heterogeneous rate constant ($k^{o'}$) of electron transfer [44,46–48].

Table 1 Electrochemical parameters of Mb(III)/Fe(II) redox couples.

Media	Electrode	$-E^{0'}$ V vs. SCE	10^3D $cm^2\ s^{-1}$	$10^{-3}\ k^{o'}$ cm s^{-1}
SDS[a]	GC[b]	0.18 ± 0.013		0.063 ± 0.020
	Pt[c]	0.562 ± 0.018	2.5	0.021 ± 0.012
CTAB[d]	GC[b]	0.189 ± 0.0155		0.033 ± 0.019
	Pt[c]	0.611 ± 0.008	1.4	0.0083 ± 0.0027

[a]Sodium dodecyl sulfate microemulsion.
[b]Glassy carbon electrode.
[c]Pt electrode.
[d]Cetyltrimethylammonium bromide microemulsion.

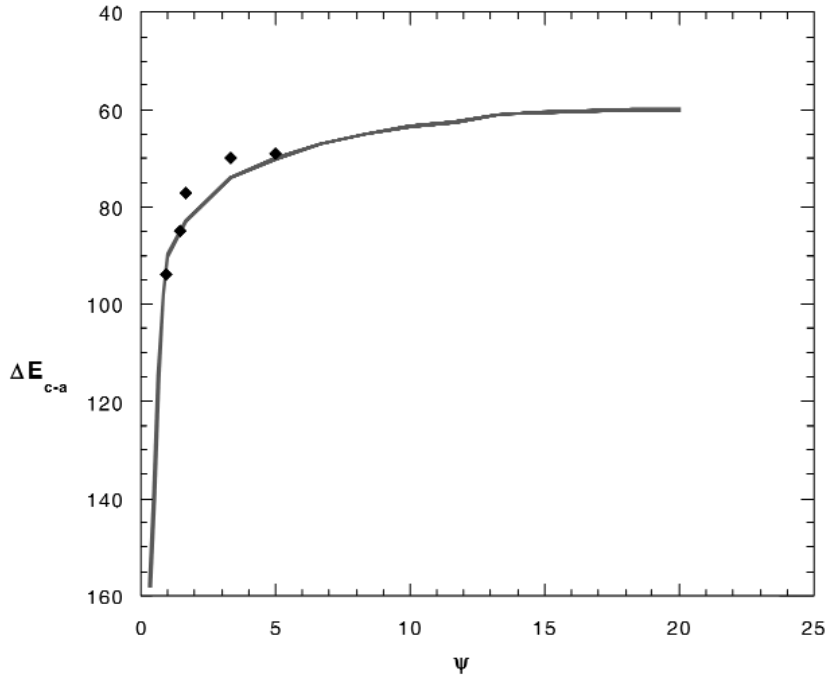

Fig. 4 Theoretical working curve for ΔE vs. ψ, where $\psi = (D_O/D_R)^{\alpha/2}\, k^{o'}/(\Pi nFvD_O/RT)^{1/2}$. The line represents the theoretical curve, whereas dots represent the experimental values.

CATALYTIC REDUCTION OF DBCH AND TCA

Reactions of the reduced form of the Mb, i.e., MbFe(II), with DBCH (example of alkyl vicinal dihalides) is a case of inner-sphere electron-transfer reaction, which means bonds are formed or cleaved within the time scale of the experiment [28,29,31,46]. Upon addition of DBCH (60 mM) to a solution containing Mb(III), cathodic currents in excess of those in absence of DBCH were obtained at both GC and Pt electrodes (Fig. 5). No shift in potential was observed, contrary to what was observed for vitamin B_{12}-DBCH-DDAB microemulsion system [31]. Moreover, large currents were obtained for the reduction of Mb in the presence of TCA at Pt electrodes. No reverse peak was observed except at scan rates exceeding 2 V s^{-1}, suggesting a fast reaction of MbFe(II) species with DBCH in microemulsions. In SDS and CTAB microemulsions, direct reduction of DBCH occurs at –1.86 ± 0.003 V vs. SCE, at a sweep rate of 0.2 V s^{-1}, with no anodic peak, which is more negative than the MbFe(III)/Fe(II) couple by about 1.4 V. Similar results were obtained for direct reduction of TCA, whose peak potential was about –1.7 V vs. SCE. The measured current varied linearly with the scan rate.

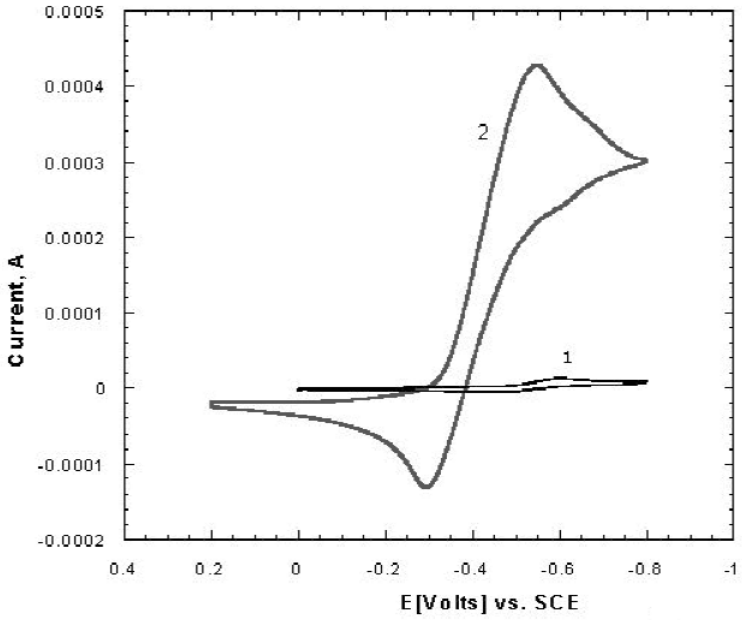

Fig. 5 Cyclic voltammogram of 0.07 mM metMb in SDS microemulsion at 0.05 V s^{-1} at Pt electrode with (1) no added TCA; (2) 20 mM TCA added.

Current efficiency

The current efficiency $(I_c/I_d)_s$ defined as the ratio of the current in the presence (I_c) and absence of the substrate (I_d), at a potential of the catalyst in absence of the substrate, decreased with the scan rate, at GC electrodes (Table 2), as expected. However, it remained relatively constant at Pt electrodes, with an average value of 2.22 ± 0.42 for DBCH/SDS/Pt and 3.29 ± 0.76 for DBCH/CTAB/Pt system. Results for catalytic reduction of DBCH were similar in SDS and CTAB microemusions at GC electrodes. When 20 mM trichloroacetic acid was added to metmyoglobin in SDS and CTAB microemulsion, a large increase in MbFe(III)/Fe(II) reduction current was observed at both GC and Pt electrodes (Fig. 5). The oxidation peak for MbFe(III)/Fe(II) decreased significantly, and the overall reduction potential of the catalyst shifted slightly to more positive values, due to decrease in pH. Direct reduction of TCA occurs at –1.7 V vs. SCE, suggesting a lowering of overpotential for the reduction of TCA by about 1.3 V, which is an energy-saving factor for decomposition of organohalides and electrosynthesis for starting materials in industries. The increase in current for TCA/CTAB/GC is about twice that observed for TCA/SDS/GC (Table 2). The catalytic current (I_c) decreased with increase in scan rate in case of GC, as expected, but remained relatively constant in the case of Pt electrodes (Table 2).

Table 2 Variation of catalytic efficiency (I_c/I_d) with the scan rate, type of media, substrate (DBC or TCA) and type of electrode.

	SDS/GC		SDS/Pt		CTAB/G		CTAB/Pt	
ν	DBCH	TCA	DBC	TCA	DBC	TCA	DBC	TCA
V s^{-1}	60 mM	20 mM	60 mM	20 mM	60 mM	20 mM	60 mM	20 mM
0.01	2.13	2.72	–	–	–	–	–	–
0.015	–	–	1.90	56.2	2.44	5.69	5.38	38.0
0.025	2.06	3.32	2.62	63.6	2.55	5.88	3.22	36.5
0.05	2.00	3.02	2.08	–	1.93	4.56	3.21	35.0
0.1	1.68	–	2.01	53.6	1.79	3.85	3.55	35.6
0.2	1.37	1.70	1.87	47.7	1.85	2.71	2.80	29.9
0.3	1.03	1.31	2.02	50.2	1.13	1.70	3.26	31.2
0.5	1.01	1.29	2.05	52.1	1.28	1.45	3.26	25.7
0.6	1.08	1.11	–	–	–	–	–	–
0.8	–	–	3.18	38.5	1.36	1.46	2.92	37.9
1.0	0.83	0.88	–	41.0	1.18	1.19	2.41	39.0
1.5	–	–	–	–	1.08	1.14	2.51	44.7
1.6	–	–		39.7	–	–	–	–
2.0	0.82	0.88	–	–	1.16	1.12	3.63	32.2
3.0	0.89	0.91	–	44.0	1.09	1.2	–	–
5.0	–	0.98	–	–	–	–	–	–

Catalytic decomposition of organohalide

The organohalide decomposition pathway, Scheme 1, proposed for the catalytic reduction of alkyl halides in organic solvents and water in oil microemulsions [28–31,34,43,46], using porphyrin metal complexes, was tested for SDS and CTAB data at GC electrodes.

$$\text{MbFe(III)} + \text{e} \rightleftarrows \text{MbFe(II)}\ k^{o\prime} \tag{1}$$

$$\text{MbFe(II)} + \text{RX} \rightarrow \text{MbFe(III)} + \text{intermediates}\ k', \text{rds} \tag{2}$$

$$\text{MbFe(II)} + \text{intermediates} \rightarrow \text{MbFe(III)} + \text{alkene} + \text{halide} \tag{3}$$

Scheme 1

According to Scheme 1, the active form of the catalyst, MbFe(II), formed at the surface of the electrode (eq. 1), reacts with either DBCH (RX2) or TCA (RX3) in the rate-determining step (rds, eq. 2). Equation 2 yields the intermediates and regenerates the catalyst, MbFe(III), which is recycled at the electrode surface, thereby increasing the reduction current [44,46], now called the catalytic current (I_c). The intermediates can be reduced by MbFe(II) in a solution electron transfer (SET, three-dimensional electron distribution, in the sense that electron is no longer restricted to move in one dimension only as in the case of electron from the electrode) or in an adsorbed electron transfer (AET) microenvironment. This step further increases the catalytic current. The rate-determining step involves the bimolecular reaction of MbFe(II) with RX2 or RX3, where X is bromide ion in the case of DBCH or X is chlorine in the case of trichloroacetic acid. The ratio of the catalytic current (I_c) in the presence of the substrate (DBCH or TCA) to the current in the absence of the substrate (I_d) is known as the catalytic efficiency (CE), symbolized I_c/I_d. Variation of catalytic efficiency with scan rate (v) is used to estimate the rate constant (k') of the rate-determining step (rds) of the overall reaction [44,46–48]. A theoretical working curve of I_c/I_d vs. $\lambda^{1/2}$, where $\lambda = 0.02567[\text{substrate}]k'/v$, was used to estimate k' (Fig. 6). For a given media and substrate, k' was relatively constant at different scan rates, as demonstrated by stan-

dard deviations of at least ±10 % (Table 3). Goodness of fit of Scheme 1 to the data is found from the agreement of the experimental values (I_c/I_d) ploted using the average k' with the theoretical curve (Fig. 6). Both SDS and CTAB microemulsions showed good agreement with the theoretical curve.

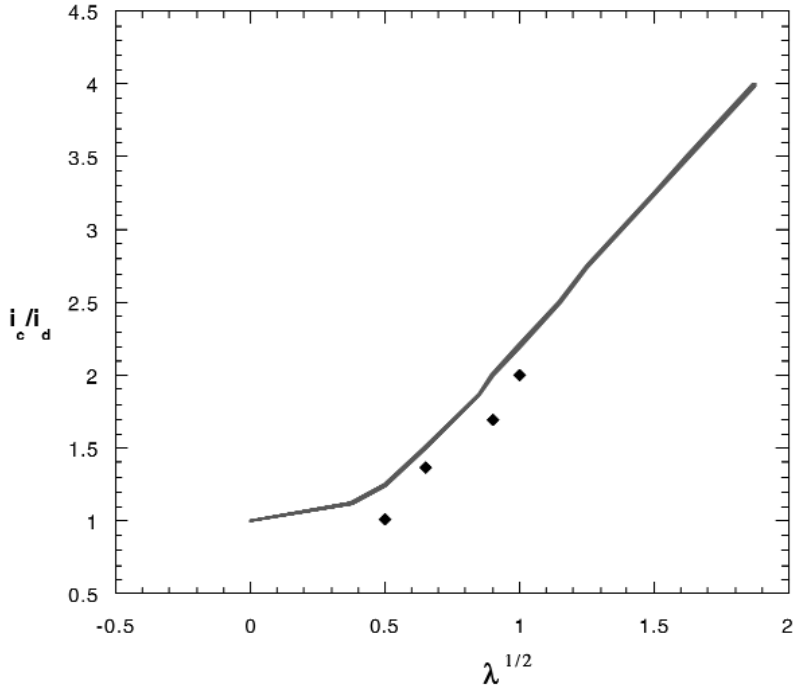

Fig. 6 Catalytic efficiencies I_c/I_d vs. $\lambda_{1/2}$, where $\lambda = \{0.0256762[\text{substrate}]k'/v\}$. k' is the rate constant and v is the scan rate in V s^{-1}. The line represents theoretical curve, whereas dots represent experimental values.

Table 3 Rate constants[a] for reduction of DBCH and TCA by metMb in SDS and CTAB microemulsions.

Media	Substrate	10^{-3} k', M^{-1} s^{-1}	ΔE/V[b]
SDS	DBCH	0.041 ± 0.01	1.57
	TCA	0.48 ± 0.10	1.37
CTAB	DBCH	0.15 ± 0.016	1.56
	TCA	2.75 ± 0.67	1.36

[a]Rate constant for the reaction (rds) between the catalyst and the substrate.
[b]$\Delta E = -E^{0\prime}$(metMbFe(III)/Fe(II) - $E_{1/2}$ (substrate, DBCH or TCA). Results obtained from GC electrode only.

DISCUSSION

In aqueous solutions, catalytic hydrogen evolution usually occurs at potentials more positive than –0.5 V vs. SCE at Pt electrodes. However, this work demonstrated that aqueous microemulsions of SDS and CTAB are capable of expanding the working potential window of Pt electrode up to about –2.0 V vs. SCE. This was attributed to restricted microenvironment created by the water and oil channels, making H^+ ions in water conduits unavailable for reduction at Pt electrode. The ability of the microemulsion

to form compartments of varying polar zones enabled investigation of Mb in both solution form and adsorbed form at different electrodes.

Data for reactions of MbFe(III)/Fe(II) redox couples with DBCH and TCA in bicontinuous SDS and CTAB microemulsions were consistent with Scheme 1. The results compare favorably with those obtained earlier, where Mb was adsorbed onto didodecyldimethylammonium bromide (DDAB) films at pH 5.5 acetate buffer [26,33]. Moreover, the results compared well with those obtained at DDAB microemulsions, where copper and nickel were used as the catalysts [9]. On the other hand, the rate constants were significantly lower than those obtained for catalytic reduction of TCA by vitamin B_{12}Co(I) in homogeneous acetonitrile water [26,30]. The lower catalytic efficiencies ($I_c/I_d < 5$ at carbon electrodes) may be rationalized on the basis that theoretically catalytic currents decrease when the standard potential of the redox catalyst becomes less negative [28]. The current work is a case of high positive values for reduction of the catalyst, relative to that of the substrate, demonstrating high lowering of overpotential for the reduction of DBCH and TCA at GC electrodes. But in the case of Pt electrode, the redox potential of the catalyst is more negative than that at GC, by about 300 mV, which partially explains the increase in catalytic efficiency at this electrode. Moreover, at this point one cannot rule out completely the slight influence of catalytic hydrogen evolution in the presence of substrate, particularly for the reduction of TCA at Pt, even though this was not observed for direct reduction of substrate in the absence of MetMbFe(III)/Fe(II) couple. According to Table 2, the behavior for catalytic reduction of DBCH is relatively similar in both SDS and CTAB microemulsions at both electrodes (GC and Pt). However, catalytic efficiencies for TCA were significantly higher than that of DBC in both SDS and CTAB microemulsions. This is attributed to the fact that TCA is polar relative to DBCH and therefore it resides in the water channels, in the vicinity of the myoglobin, which is also polar, thereby enhancing the reaction rates of the two reactants. DBCH resides exclusively in the oil channel or in the interfaces occupied by the surfactants, and therefore its reaction with catalyst is constrained to some extent. Close scrutiny of the data (Table 2) indicates that catalytic efficiency for reduction of TCA in CTAB is about twice that in SDS microemulsion at GC electrodes. This may be rationalized on the fact that the positive surface charge on the surfactant (CTAB) stabilizes the reduced form of the polar TCA intermediates and MbFe(II) much more than the negatively surface charged SDS surfactant.

The significantly higher value of k' obtained in TCA/CTAB system suggests influence of positive surface charge of the surfactant on the products. Definitely, the positive charge on CTAB microemulsion is expected to stabilize the X^- ions produced, more strongly than the negatively charged SDS microemulsion.

CONCLUSIONS

Microemulsions made of SDS and CTAB gave reversible MbFe(III)/Fe(II) voltammetry at GC, PG, and Pt electrodes. Reactions at GC and PG occur via a thin layer of adsorbed catalyst on the surface of the electrode. The adsorbed films were stable for several weeks. On the other hand, reactions at Pt electrodes gave diffusion-controlled peaks, demonstrating a thick adsorbed layer of Mb-surfactant on the surface of electrode. Catalytic reduction of DBCH and TCA occurred at around –0.2 V vs. SCE, whereas direct reduction of DBCH and TCA occurs at potentials more negative than –1.7 V vs. SCE. This gives a lowering of decomposition potential for DBCH and TCA of about 1.4 V, which is a significant saving of energy. This work demonstrates the use of SDS and CTAB microemulsions as a media for solubilization of Mb, which is known to be sensitive to different media due to denaturing properties. The catalytic efficiencies decreased with the scan rate as expected with other media. The blue shift of soreto band of Mb in SDS microemulsion, by 8 nm, relative to what is observed in water (acetate buffer) indicates that the catalyst is in a microenvironment different from that of water alone, pointing a finger to residency in interstitial sites occupied by the surfactant. The results showed subtle significant differences between SDS and CTAB microemulsion, signifying the possibility of designing microassembly

for a specific need. The extended range for working potential of platinum, without hydrogen evolution, demonstrated ability of microemulsion to "shut off" interfering signals for a specific reaction.

ACKNOWLEDGMENT

The authors wish to thank NSF and University of Connecticut for supporting this work.

REFERENCES

1. J. F. Rusling and C. J. Campbell. "Electrochemical reactions in microemulsion", *Encyclopedia of Surface and Colloid Science*, Marcel Dekker, New York (2002).
2. S. Friberg. *Adv. Colloid Interface Sci*. **32**, 167–182 (1990).
3. P. G. Wislocki, G. T. Miwa, A. Y. H. Lu. In *Enzymatic Basis of Detoxication*, W. B. Jakoby (Ed.), Academic Press, New York (1980).
4. F. P. Guengerich and T. L. MacDonald. *Acc. Chem. Res*. **17**, 9–16 (1984).
5. J. F. Rusling. *Acc. Chem. Res*. **24**, 75–81 (1991).
6. J. F. Rusling. In *Electroanalytical Chemistry*, Vol. 18, A. J. Bard (Ed.), pp. 1–88, Marcel Dekker, New York (1994).
7. J. F. Rusling. In *Modern Aspects of Electrochemistry*, No. 26, B. Conway and J. O'M. Bockris (Eds.), pp. 49–104, Plenum Press, New York (1994).
8. R. A. Mackay. *Colloids Surf*. **82**, 1–23 (1994).
9. G. N. Kamau, N. Hu, J. F. Rusling. *Langmuir* **8**, 1042–1044 (1992).
10. G. N. Kamau and J. F. Rusling. *J. Electroanal. Chem. Inter. Electrochem.* **240**, 217–226 (1988).
11. G. N. Kamau, T. Leipert, S. S. Shukla, J. F. Rusling. *J. Electroanal. Chem. Inter. Electrochem.* **233**, 173–187 (1987).
12. (a) F. D. Blum, S. Pickup, B. W. Ninham, S. J. Chen, D. F. J. Evans. *J. Phys. Chem*. **89**, 711–713 (1985); (b) S. J. Chen, D. F. Evans, B. Ninham, D. J. Mitchell, D. J. Blum, F. D. Pickup. *J. Phys. Chem*. **90**, 842–847 (1986).
13. M. O. Iwunze, A. Sucheta, J. F. Rusling. *Anal. Chem*. **62**, 644–649 (1990).
14. M. O. Iwunze and J. F. Rusling. *J. Electroanal. Chem*. **303**, 267–270 (1991).
15. P. R. Ortiz de Montellano and C. E. Catalano. *J. Biol. Chem.* **260**, 9265–9271 (1985).
16. A. Arduini, L. Eddy, P. Hochstein. *Arch. Biochem. Biophys*. **281**, 41–43 (1990).
17. D. J. Kelman, J. A. DeGray, R. P. Mason. *J. Biol. Chem*. **269**, 7458–7463 (1994).
18. R. S. Wade and C. E. Castro. *J. Am. Chem. Soc*. **95**, 231–234 (1973).
19. E. W. Bartnicki, N. O. Belser, C. E. Castro. *Biochemistry* **17**, 5582–5586 (1978).
20. I. Homachi, S. Noda, T. Kunitake. *J. Am. Chem. Soc*. **113**, 9625–9630 (1991).
21. J. F. Rusling and A.-E. F. Nassar. *J. Am. Chem. Soc*. **115**, 11891–11897 (1993).
22. P. R. Ortiz de Montellano (Ed.). *Cytochrome P450*, Plenum Press, New York (1986).
23. R. Scheffold. *Chimia* **39**, 203–211 (1985).
24. S. Busato, O. Tinembart, Z. Zhang, R. Scheffold. *Tetrahedron* **46**, 3155–3166 (1990).
25. T. F. Connors, J. V. Arena, J. F. Rusling. *J. Phys. Chem.* **92**, 2810–2816 (1988).
26. A.-E. F. Nassar, J. M. Bobbitt, J. D. Stuart, J. F. Rusling. *J. Am. Chem. Soc*. **117**, 10986–10993 (1995).
27. R. S. Wade, R. Havlin, C. E. Castro. *J. Am. Chem. Soc.* **91**, 7530 (1969).
28. D. Lexa, J. M. Saveant, K. B. Su, D. L. Wang. *J. Am. Chem. Soc.* **109**, 6464–6470 (1987).
29. D. Lexa, J. M. Saveant, K. B. Su, D. L. Wang. *J. Am. Chem. Soc.* **110**, 7617–7625 (1988).
30. A. Owlia, Z. Wang, J. F. Rusling. *J. Am. Chem. Soc*. **111**, 5091–5098 (1989).
31. D.-L. Zhou, J. Gao, J. F. Rusling. *J. Am. Chem. Soc.* **117**, 1127–1134 (1995).
32. J. F. Rusling, C. L. Miaw, E. C. Couture. *Inorg. Chem*. **29**, 2025–2027 (1990).

33. (a) A.-E. F. Nassar, W. S. Wills, J. F. Rusling. *Anal. Chem.* **67**, 2386–2392 (1995); (b) J. F. Rusling and A.-E. F. Nassar. *Langmuir* **10**, 2800–2806 (1994).
34. (a) D. Zhou, C. K. Njue, J. F. Rusling. *J. Am. Chem. Soc*. **121**, 2909–2914 (1999); (b) J. Georges and J. W. Chen. *Colloid Polym. Sci.* **264**, 896–902 (1986).
35. D. Voet and J. G. Voet. *Biochemistry*, 2nd ed., John Wiley, New York (1995).
36. (a) D. Galaria, L. Eddy, A. Arduini, E. Cadenas, P. Hochstein. *Biochem. Biophys. Res. Commun.* **160**, 1162–1168 (1989); (b) A. C. Onuoha, X. Zu, J. F. Rusling. *J. Am. Chem. Soc.* **119**, 3979–3986 (1997).
37. J. J. O. Turner, C. A. Rice-Evans, M. J. Davies, E. S. R. Newman. *Biochem. J.* **277**, 833–837 (1991).
38. J. J. O. Turner, C. A. Rice-Evans, M. J. Davies, E. S. R. Newman. *Biochem. Soc*. *Trans*. **18**, 1056–1059 (1990).
39. C. K. Njue and J. F. Rusling. *J. Am. Chem. Soc*. **122**, 6459–6463 (2000).
40. R. A. Mackay, S. A. Myers, A. Brajter-Toth. *Electroanalysis* **8**, 759–764 (1996).
41. J. Georges, J. W. Chen, N. Anoud. *Colloid Polym. Sci*. **265**, 45–51 (1987).
42. M. Clausse, J. Heil, J. Peyrelasse, C. Boned. *J. Colloid Interface Sci*. **87**, 584–586 (1982).
43. J. F. Rusling and A.-E. F. Nassar. *J. Am. Chem*. **115**, 11891–11897 (1993).
44. A. J. Bard and L. R. Faulkner. *Electrochemical Methods*, John Wiley, New York (1980).
45. I. Taniguchi, K. Watanabe, M. Tominaga, F. Hawkridge. *J. Electroanal. Chem*. **333**, 331–338 (1992).
46. D. Lexa, J. M. Saveant, H. J. Schafer, K.-B. Su, B. Vering, D. L. Wang. *J. Am. Chem. Soc.* **112**, 6163–6177 (1990).
47. R. S. Nicholson and I. Shain. *Anal. Chem*. **36**, 706–723 (1964).
48. R. S. Nicholson. *Anal. Chem.* **37**, 1351–1355 (1965).